Two central pattern generators from the crab, *Cancer borealis*, respond robustly and differentially to extreme extracellular pH

Jessica A. Haley[†], David Hampton, Eve Marder*

Volen Center and Biology Department, Brandeis University, Waltham, MA 02454

* **Corresponding Author:**
marder@brandeis.edu

[†] **Current Address:**
Neurosciences Graduate Program, University of California San Diego, La Jolla, CA 92037

Running title:
Effects of pH on crab central pattern generating networks

Author contributions:
Conceptualization, E.M.; **Data Curation**, J.A.H. and E.M.; **Formal Analysis**, J.A.H. and D.H.; **Funding Acquisition**, E.M.; **Investigation**, J.A.H. and D.H.; **Methodology**, J.A.H.; **Project Administration**, E.M.; **Resources**, E.M.; **Software**, J.A.H.; **Supervision**, E.M.; **Validation**, J.A.H.; **Visualization**, J.A.H.; **Writing – Original Draft Preparation**, JA.H. and D.H.; **Writing – Review & Editing**, J.A.H., D.H., and E.M.

Abbreviations:
STG, stomatogastric ganglion; **CG**, cardiac ganglion; **CPG**, central pattern generator; **AB**, Anterior Burster; **PD**, Pyloric Dilator; **LP**, Lateral Pyloric; **PY**, Pyloric; **SC**, Small Cell; **LC**, Large Cell; **lvn**, lateral ventricular nerve; **PTX**, picrotoxin; **IPSP**, inhibitory post-synaptic potential; **LG**, Lateral Gastric; **MG**, Medial Gastric; **LPG**, Lateral Posterior Gastric; **GM**, Gastric Mill; **DG**, Dorsal Gastric; **AM**, Anterior Median; **Int1**, Interneuron 1; **mvn**, medial ventricular nerve; **dgn**, dorsal gastric nerve; **lgn**, lateral gastric nerve; **ion**, inferior oesophageal nerve; **IC**, Inferior Cardiac; **VD**, Ventricular Dilator; **MCN1**, Modulatory Commissural Neuron 1; **VCN**, Ventral Cardiac Neuron; **CPN2**, Commissural Projection Neuron 2; **CoG**, commissural ganglion

Abstract

Most animals and their neuronal circuits must maintain function despite significant environmental fluctuations. The Jonah crab, *Cancer borealis*, experiences daily changes in ocean temperature and pH which are becoming more extreme as rises in atmospheric carbon dioxide continue to increase ocean temperature and contribute to ocean acidification. Here, we describe the effects of extreme changes in extracellular pH on two central pattern generating networks of the stomatogastric (STG) and cardiac (CG) ganglia of *C. borealis*. We examined the activity of the pyloric rhythm of the STG and the cardiac rhythm of the CG using extracellular and intracellular electrodes as bath superfused saline was shifted from pH 5.9 to pH 11.0. Given that the physiological properties of ion channels are known to be sensitive to pH within the range tested, it is surprising that the pyloric rhythm generally remained robust from pH 6.4 up to pH 9.6. Intracellular recordings of two of the pyloric neurons, the Lateral Pyloric and Pyloric Dilator, revealed depolarization of the membrane potential in extreme pH. Similarly, the cardiac rhythm retained robust activity across nearly the entire range of pH. Surprisingly, the STG was more sensitive to acid and the CG was more sensitive to base. We reveal considerable animal-to-animal variability in response to extreme perturbations, likely a consequence of the fact that similar network performance can arise from variable sets of underlying conductances. Together, these results illustrate the potential difficulty in generalizing the effects of environmental perturbation across circuits, even within the same animal.

Introduction

Nervous systems must be both robust and adaptable to changes in internal and external conditions. Many intertidal marine crustaceans, such as the crabs and lobsters inhabiting the North Atlantic, experience large fluctuations in ocean temperature, acidity, dissolved oxygen levels, and salinity. The Jonah crab, *Cancer borealis*, can often be found foraging for food in intertidal zones where it experiences temperatures between 3°C and 24°C with fluctuations as great as 10°C in a single day [1-3]. As pH is a temperature-dependent measure, ocean pH fluctuations occur over the daily, monthly, and yearly experiences of long-lived crustaceans, such as *C. borealis*.

Increased atmospheric carbon dioxide is causing rises in both the temperature [4, 5] and dissolved carbon dioxide concentration of the world's oceans [6, 7]. If current trends continue, estimates reveal that these changes will reduce the average ocean pH from 8.1 to 7.6 in the next century [8]. The effects of ocean acidification are noticeably disrupting marine ecosystems, killing coral and reducing the integrity of crustacean shells [9, 10]. In the lobster, *Homarus americanus*, prolonged thermal stress results in pH acidosis, hyperchloremia, and hyperproteinemia [11] and has been linked to mortality [12]. Further, shifts in hemolymph pH *in vitro* alter the frequency and strength of the lobster cardiac rhythm [13].

In several marine invertebrates including *H. americanus* and the crab, *Carcinus maenas*, hemolymph pH varies inversely with temperature following the rules of constant relative alkalinity [11, 13-17]. In other words, as temperature increases, hemolymph acidifies by approximately -0.016 pH/°C to maintain a constant ratio of pH to pOH through a process of bicarbonate buffering. Maintenance of this ratio in extra- and intracellular fluids is thought to be important for stabilizing macromolecular

25 structure and function [18-21]. Like hemolymph, intracellular pH generally decreases as
26 temperature rises, but has been shown to change at varying rates in different tissues in
27 the crab, *Callinectes sapidus* [17].

28 Both temperature and pH alter the biophysical parameters governing the activity
29 of ion channels and pumps in excitable membranes. Studies on the biophysical effects of
30 pH on ion channels revealed attenuation of sodium, calcium, and potassium currents
31 under acidic extracellular conditions [22-27]. In the frog myelinated nerve, changing
32 extracellular saline from pH 7 to pH 5 reduces sodium currents by up to 60% in a
33 membrane potential-dependent manner [28] which may be mediated by increased
34 sodium channel inactivation [29]. In rat CA1 neurons, moderate pH shifts from 7.4 to
35 6.4 reversibly depressed and shifted the voltage dependence of sodium (15%
36 attenuation; +3 mV shift) and calcium currents (60% attenuation; +8 mV shift) and
37 shifted potassium current inactivation to more depolarized voltages (+10 mV) while
38 moderate alkalosis up to pH 8.0 had the opposite effect [24]. Studies suggest that
39 protonation of an acidic group with pK_a between 5.2 and 7.1 causes this reversible gating
40 of sodium, calcium, and potassium channels [24]. Decreases in glutamatergic synaptic
41 function [30-32] and increases in GABAergic synaptic function [33] in response to
42 decreases in pH have been shown.

43 Although the biophysical, ethological, and environmental implications of
44 changing pH have been well studied, little is known about the effect of pH changes on a
45 neuronal circuit. Here, we study the effects of acute changes in extracellular pH on two
46 well characterized neuronal circuits, the stomatogastric (STG) and cardiac (CG) ganglia,
47 of the crab, *C. borealis*. These central pattern generators (CPGs) drive the coordinated
48 and rhythmic muscle movements of the crab's stomach and heart, respectively [34].

Although these CPGs are driven by numerically simple neuronal circuits, their dynamics involve complex interactions between many intrinsic and synaptic currents. By studying the rhythmic activity of the STG and CG in response to global perturbation, we reveal generalizable principles for network robustness.

Previous studies have shown that the pyloric rhythm of the STG and cardiac rhythm of the CG are remarkably robust to short- and long-term changes in temperature in both *in vivo* and *ex vivo* preparations [35-37]. Despite similarly robust activity under moderate perturbation, these experiments have revealed animal-to-animal variability in network activity at extreme temperatures [35, 36]. In accordance with these findings, we reveal that both the pyloric and cardiac rhythms are remarkably robust to acute pH changes from 5.9 to 11.0. This is surprising given the sensitivity of many ion channels to pH in these ranges and suggests that networks can be more robust to pH changes than their component ion channels.

Results

Figure 1 introduces the two neuronal networks studied in this paper. The stomatogastric ganglion (STG) of the crab, *Cancer borealis*, is a central pattern generating circuit that produces rhythmic motor patterns. The pyloric rhythm is driven by a three-neuron pacemaker kernel – one Anterior Burster (AB) and two Pyloric Dilator (PD) neurons. The Lateral Pyloric (LP) and Pyloric (PY) neurons fire out of phase with the PD neurons because they are rhythmically inhibited by the PD/AB group. The cardiac ganglion (CG) of *C. borealis* is another rhythmic motor circuit containing four pacemaker Small Cell (SC) neurons that drive five motor Large Cell (LC) neurons.

Fig 1. Preparations and circuit diagrams.

(A) Schematic of the stomatogastric nervous system preparation. Extracellular electrodes were placed in vaseline wells (gray circles) drawn around nerves of interest. An example extracellular nerve recording from the lateral ventricular nerve (lvn) shows two cycles of the triphasic pyloric rhythm containing spikes from the lateral pyloric (LP), pyloric (PY), and pyloric dilator (PD) neurons. Example intracellular recordings from the LP and PD neurons are displayed. Simultaneous pH recording was achieved using a pH microelectrode placed near the ganglion. (B) Simplified diagram of the pyloric circuit. Filled circles represent inhibitory chemical synapses; resistor symbols represent electrical coupling. (C) Schematic of the cardiac ganglion preparation. Extracellular electrodes were placed in a well (gray circle) around the trunk of the preparation. An example extracellular recording shows one burst of the pacemaker Small Cell (SC) and motor Large Cell (LC) neurons. (D) Diagram of the cardiac circuit. Filled triangles

85 represent excitatory chemical synapses; the resistor symbol represents electrical
86 coupling.
87
88 Figure 1A shows a schematic diagram of our preparation of the stomatogastric
89 nervous system. Intracellular recordings were made from the somata of the desheathed
90 STG. Examples are shown of the waveforms of the LP and PD neurons. Vaseline wells
91 were placed on the motor nerves at the indicated sites to obtain extracellular recordings
92 of the STG fictive motor patterns. An example of the activity of the triphasic activity of
93 the LP, PD, and PY neurons are seen in the inset trace next to the lateral ventricular
94 nerve (lvn) electrode. Figure 1B gives the connectivity diagram of the major neuron
95 classes of the triphasic pyloric rhythm.
96 Figure 1C shows a schematic diagram of our preparation of the crab cardiac
97 ganglion. SC and LC activity of the cardiac ganglion were recorded from the trunk. The
98 inset shows an example of one burst of SC and LC rhythmic activity. Figure 1D gives the
99 connectivity diagram of the cardiac ganglion.
100
101 ***The Pyloric rhythm is surprisingly robust to extreme changes in pH***
102 To characterize the response of the pyloric rhythm to acute changes in pH, the
103 pH of superfused saline was changed every 15 minutes in steps of approximately pH 0.5
104 from a control pH of 8.2 to an extreme pH of either 5.9 or 11.0. Following the first acid
105 or base step protocol, the preparation was allowed to recover for a minimum of 30
106 minutes at control pH until the frequency of the pyloric rhythm approached that of
107 controls. The preparation was then subjected to a step protocol in the opposite direction
108 preceding a second recovery period. Acid- or base-first protocols were counterbalanced.

109 Figure 2 shows an example experiment with an acid-first protocol. Each box
110 contains example traces from the last minute of each pH condition. Intracellular
111 recordings of the PD and LP neurons and extracellular recordings of the lvn are shown.
112 In the top row of Figure 2, the preparation started in control saline at pH 8.2 and
113 demonstrated a normal triphasic rhythm. As the preparation was subjected to more
114 acidic saline, the rhythm remained triphasic until the most acidic pH, 5.9. Control
115 activity was recovered when the preparation was once again placed in control saline, as
116 seen in the top right panel. The bottom row of Figure 2 shows the same preparation in
117 basic conditions. As the preparation was subjected to pH 11.0 saline, it remained
118 triphasic, although with fewer spikes per burst and lower amplitude slow waves. Again,
119 the preparation returned to a more canonical triphasic rhythm in control saline as seen
120 in the bottom right box.
121
122 **Fig 2. Robust pyloric rhythm activity across pH.**
123 Example stomatogastric ganglion experiment with an acid-first protocol. Each colored
124 box displays five seconds of recordings taken from the last minute at each pH step.
125 Intracellular recordings of the PD and LP neurons and extracellular recordings of the
126 lvn are shown. The experiment can be read left to right then top to bottom in
127 chronological order. Horizontal lines indicate a reference membrane potential of -40
128 mV; vertical lines indicate a scale of 10 mV.
129
130 While some preparations maintained surprisingly robust pyloric rhythms from
131 pH 5.9 to 11.0, others exhibited compromised patterns of activity at the most extreme
132 pH levels. Figure 3A shows the activity of two preparations across the range of pH

133 tested. Intracellular recordings of PD neurons with synchronous extracellular recordings
134 of the lvn are shown. Both preparations display robust activity across a nearly three-fold
135 range of hydrogen ion concentration but become weakly active or silent at pH 5.9. At pH
136 11.0, STG #2 is weakly triphasic and considerably slower than it was at pH 8.2 while
137 STG #3 retains a strong triphasic rhythm. These examples highlight both the animal-to-
138 animal variability of the pyloric rhythm at control conditions and the variable effects of
139 extreme acidosis or alkylosis on this network.
140
141 **Fig 3. Variability of pyloric rhythm activity at extreme pH.**
142 (A) Two additional stomatogastric ganglion experiments displaying three seconds of
143 intracellular PD and extracellular lvn recordings. Horizontal lines indicate a reference
144 membrane potential of -40 mV; vertical lines indicate a scale of 10 mV (B) Five states
145 were defined to characterize pyloric rhythm activity. Examples of activity for each state
146 are given. (C) Stacked bars give the mean fraction of time that all 15 preparations spent
147 in each state over the last eight minutes of each pH step. As pH 8.2 was used as a control
148 prior to each ramp and as a recovery after each ramp, four bars for pH 8.2 are shown to
149 maintain the chronology of the protocol; recovery at pH 8.2 after exposure to pH 5.9
150 and 11.0 are shown on the far left and far right, respectively. Asterisks denote statistical
151 significance revealed by paired samples t-tests with Bonferroni correction (* $p < 0.05$; **
152 $p < 0.01$; *** $p < 0.001$).
153
154 To characterize these effects across all preparations, we defined five states of
155 activity: 1) 'normal triphasic' rhythm containing PD, LP, and PY with a minimum of
156 three spikes per burst for each unit; 2) 'weak triphasic' rhythm retaining all 3 units with

157 some units spiking only once or twice per cycle; 3) 'intermittent triphasic' rhythm
158 describing rhythmic activity with only some units active; 4) 'all silent'; and 5) 'atypical
159 activity' or activity that could not be categorized under the first four definitions (Fig 3B).
160 Preparations were categorized systematically according to the criteria outlined in
161 Materials and Methods. Figure 3C shows the mean fraction of time that all preparations
162 spent in these five states at steady state (i.e. during the last eight minutes of each step of
163 pH). A One-Way Repeated-Measures ANOVA of the effect of pH on the fraction of time
164 the preparations were rhythmic (i.e. a combined metric of states 1 – normal triphasic –
165 and 2 – weak triphasic) revealed a significant effect of acid (F (4,56) = 33.466, $p <$
166 0.0001) and base ($F(5,70) = 7.451$, $p < 0.0001$) on the pyloric rhythm. Paired samples t-
167 tests with Bonferroni correction confirm that the fraction of time the preparations were
168 rhythmic was significantly less at pH 5.9 ($t(14) = 9.858$, $p < 0.0001$) and pH 11.0 ($t(14)$
169 $= 3.688$, $p = 0.0122$) compared to control pH 8.2.
170 To describe these effects quantitatively, mean measures of rhythm frequency, the
171 number of PD spikes per burst, and PD duty cycle were calculated (Fig 4). As shown in
172 Figure 4A, the mean pyloric frequency was relatively invariant across pH values in the
173 presence of the alkaline salines ($F(5,70) = 2.245$, $p = 0.0593$), but varied significantly
174 across the acid steps ($F(4,56) = 10.941$, $p < 0.0001$). The pyloric frequency at pH 5.9 was
175 significantly slower than that at control ($t(14) = 3.370$, $p = 0.0183$). Figure 4B reveals a
176 significant effect of both acid ($F(4,56) = 32.424$, $p < 0.0001$) and base ($F(5,70) = 4.459$,
177 $p = 0.0014$) on the mean number of PD spikes per burst. The number of spikes per burst
178 was significantly reduced at pH 5.9 ($t(14) = 8.522$, $p < 0.0001$). As shown in Figure 4C,
179 there was a significant effect of acid ($F(4,56) = 26.651$, $p < 0.0001$) and base ($F(5,70) =$
180 4.442, $p = 0.0014$) on the mean PD duty cycle. Paired samples t-tests revealed a

181 decrease in PD duty cycle from control pH 8.2 to pH 5.9 ($t(14) = 5.717$, $p = 0.0002$), pH
182 9.6 ($t(14) = 3.371$, $p = 0.0228$), pH 10.1 ($t(14) = 4.787$, $p = 0.0014$), and pH 11.0 ($t(14) =$
183 4.575, $p = 0.0022$).
184
185 **Fig 4. Quantification of pyloric rhythm activity across pH.**
186 Several characteristics were computed to characterize the pyloric rhythm. Pooled data
187 across animals are plotted with vertical lines representing the standard deviation. (A)
188 Mean pyloric rhythm frequency, (B) mean number of PD spikes per burst, and (C) mean
189 PD duty cycle are plotted as a function of pH. All measures were computed as the mean
190 at steady state – the last eight minutes of each pH step. As pH 8.2 was used as a control
191 prior to each ramp and as a recovery after each ramp, four values for pH 8.2 are shown
192 to maintain the chronology of the protocol; recoveries at pH 8.2 are shown on the far
193 left and far right ends of the plot on a gray background. Asterisks denote statistical
194 significance revealed by paired samples t-tests with Bonferroni correction (* $p < 0.05$; **
195 $p < 0.01$; *** $p < 0.001$).
196
197 ***Pyloric neurons depolarize at extreme pH***
198 To determine how the intrinsic properties of isolated neurons respond to pH, we
199 analyzed several characteristics of the intracellular recordings of PD and LP neurons.
200 We isolated the neurons from most of their pyloric network synaptic inputs by blocking
201 the glutamateric inhibitory synapses with 10^{-5} M picrotoxin (PTX) (Fig 1B) [38]. Figure
202 5 shows the mean resting membrane potential (mV), spike amplitude (mV), and burst or
203 spiking frequencies (Hz) for both cells in the presence of PTX as a function of pH. In
204 Figure 5A, the waveforms of PD and LP neurons from an example preparation are

205 shown prior to PTX superfusion (leftmost traces). Note the large LP-evoked inhibitory
206 post-synaptic potentials (IPSPs) in the trough of the PD neuron waveform and the large
207 amplitude inhibition of the LP caused by activity of the PD, AB, and PY neurons.
208 Following application of PTX at control pH 8.2 (center trace), the PD neuron was still
209 bursting but the LP-evoked IPSPs were entirely blocked. Most of the inhibitory inputs to
210 the LP neuron were blocked, leaving only the cholinergic inhibition contributed by the
211 PD neurons. At pH 7.0, the PD neuron of this preparation lost most of its slow wave
212 activity and became silent and depolarized at pH 5.9. At pH 9.6, the PD burst was
213 largely intact, and at pH 11.0, the neuron showed single spike bursts. The LP neuron
214 fired tonically from pH 7.0 to 11.0, again showing loss of activity at pH 5.9 similar to PD.
215
216 **Fig 5. Intracellular characteristics of the pyloric neurons, PD and LP.**
217 Several characteristics of the PD and LP neurons in the presence of picrotoxin (PTX)
218 were measured and averaged across the last minute of each pH condition. (A) Example
219 intracellular recordings of the PD and LP neurons prior to PTX application and in the
220 presence of PTX across pH conditions. Horizontal lines indicate a reference membrane
221 potential of -40 mV; the vertical line indicates a scale of 10 mV. (B,C) Mean minimum
222 membrane potential and (D,E) mean spike amplitude are plotted for LP and PD as a
223 function of pH. (F) Mean PD burst frequency and (G) mean LP firing rate are also
224 plotted at each pH. Vertical lines at each point indicate standard deviation. Asterisks
225 denote statistical significance revealed by paired samples t-tests with Bonferroni
226 correction (* $p < 0.05$; ** $p < 0.01$; *** $p < 0.001$).
227

228 Figure 5B and 5C give pooled mean values for the most hyperpolarized levels
229 (minimum voltages) of the membrane potential for PD and LP neurons, respectively. At
230 the midrange of pH, the membrane potential was fairly stable. At extreme acid, the PD
231 neuron membrane potential depolarized substantially, while the LP neuron membrane
232 potential remained relatively constant. A One-Way Repeated-Measures ANOVA
233 confirms a significant effect of acid on PD ($F(4,32) = 34.723$, $p < 0.0001$) but not LP
234 ($F(4,32) = 1.408$, $p = 0.2535$) minimum membrane potential. In contrast, the PD
235 neuron's membrane potential in basic saline was relatively constant ($F(5,40) = 1.746$, p
236 = 0.1463), even at extreme base, but the LP neuron's membrane potential significantly
237 hyperpolarized ($F(5,40) = 46.284$, $p < 0.0001$). These results were further confirmed
238 with paired samples t-tests with Bonferroni correction revealing significant effects of pH
239 5.9 ($t(8) = 17.600$, $p < 0.0001$) and pH 6.4 ($t(8) = 4.822$, $p = 0.0053$) on PD membrane
240 potential and pH 9.6 ($t(8) = 3.978$, $p = 0.0204$), 10.1 ($t(8) = 6.031$, $p = 0.0016$), 10.6
241 ($t(8) = 7.0357$, $p = 0.0005$), and 11.0 ($t(8) = 9.981$, $p < 0.0001$) on that of LP.
242 As shown in Figure 5D and 5E, there was a slight effect of pH on spike amplitude
243 at the most extreme pH conditions for both LP and PD neurons. An ANOVA revealed a
244 significant effect of acid on PD ($F(4,32) = 26.579$, $p < 0.0001$) and LP ($F(4,32) = 8.052$,
245 $p = 0.0001$) neuron spike amplitude and base on that of LP ($F(5,40) = 3.773$, p =
246 0.0068), but not PD ($F(5,40) = 1.293$, $p = 0.2861$). Paired samples t-tests revealed
247 significant effects of pH 5.9 on both LP ($t(8) = 4.519$, $p = 0.0078$) and PD ($t(8) = 6.933$,
248 $p = 0.0005$).
249 Figure 5F shows the effect of pH on mean PD burst frequency and reveals an
250 effect of basic saline ($F(5,40) = 2.918$, $p = 0.0245$) and no significant effect in acid
251 ($F(4,32) = 1.875$, $p = 0.1390$). Figure 5E reveals the effects of pH on the mean spiking

252 frequency, firing rate (Hz), of LP neurons. LP firing rate is significantly affected by both
253 acid ($F(4,32) = 30.999$, $p < 0.0001$) and base ($F(5,40) = 29.716$, $p < 0.0001$). Paired
254 samples t-tests reveal significant reductions in LP firing rate in pH 5.9 ($t(8) = 17.264$, p
255 < 0.0001), 6.4 ($t(8) = 6.089$, $p = 0.0012$), 10.1 ($t(8) = 3.981$, $p = 0.0203$), 10.6 ($t(8) =$
256 5.147, $p = 0.0044$), and 11.0 ($t(8) = 8.832$, $p = 0.0001$).
257

258 ***Rhythmic gastric-like activity was elicited upon exposure to and recovery***
259 ***from extreme acid and base***

260 The STG contains a second slower central pattern generating circuit known as the
261 gastric mill rhythm [39]. Unlike the pyloric rhythm which contains a pacemaker kernel,
262 the gastric rhythm is controlled by the reciprocal alternation of activity of many neurons
263 driven by descending neuromodulatory inputs [39, 40]. The principal neurons involved
264 in the gastric mill rhythm are the Lateral Gastric (LG), Medial Gastric (MG), Lateral
265 Posterior Gastric (LPG), Gastric Mill (GM), Dorsal Gastric (DG), Anterior Median (AM),
266 and Interneuron 1 (Int1) neurons [41, 42].

267 The gastric mill rhythm is often absent in dissected STG preparations and
268 requires stimulation of descending and/or sensory neurons to elicit activity [43].
269 Interestingly, in 10 of 15 preparations a gastric-like rhythm appeared at pH 9.5 or above,
270 and 4 of 15 showed this type of activity in acid at or below pH 6.4. Further, a strong
271 gastric-like rhythm was elicited upon recovery from extreme acid in 5 of 15 preparations
272 and from extreme base in 7 of 15. Preparations in which gastric rhythms were seen in
273 one of these conditions were likely to display gastric-like activity in the other conditions.

274 Figure 6 shows an example preparation in control pH 8.2 as it recovers activity
275 after exposure to pH 5.9 saline. Intracellular recordings from LP and PD neurons and

276 extracellular recordings from five nerves – lateral ventricular (lvn), medial ventricular
277 (mvn), dorsal gastric (dgn), lateral gastric (lgn), and inferior oesophageal (ion) – are
278 shown. In addition to axons of the LP, PD, and PY neurons, the lvn also contains the LG
279 axon. The mvn contains axons from two neurons, the Inferior Cardiac (IC) and the
280 Ventricular Dilator (VD). Inhibition of IC and VD was coincident with LG bursting. The
281 dgn shows GM and DG activity and the lgn contains LG activity. Recordings from ion
282 reveal Modulatory Commissural Neuron 1 (MCN1) activity. One period of the gastric
283 mill rhythm can be defined by the time from the onset of one LG burst to the next.
284
285 **Fig 6. Rhythmic gastric-like activity upon recovery from extreme acid.**
286 (A) 20 minutes of recording are shown from an example experiment where the ganglion
287 had become silent at pH 5.9 and began recovering rhythmic activity in control pH 8.2
288 saline. Intracellular recordings from LP and PD neurons and extracellular recordings
289 from five nerves – lvn, mvn, dgn, lgn, and ion – are displayed. Horizontal lines indicate
290 a reference membrane potential of -40 mV; vertical lines indicate a scale of 10 mV. Gray
291 boxes correspond to the one-minute snapshots enlarged in subsequent panels (B-E)
292 respective to time. Titles of panels B-E describe the pyloric activity during and in
293 between LG bursts.
294
295 Figure 6A clearly shows an increase in both gastric and pyloric activity over time
296 with LP and PD becoming rhythmic and the emergence of strong rhythmic activity of
297 MCN1, LG, DG, and GM neurons. In Figure 6B, PD and LP neurons were silent. Strong
298 LG neuron bursts were timed with hyperpolarizations of the LP neuron. This is
299 consistent with previous findings that the neurons driving the gastric mill rhythm

300 synapse onto the pyloric network and that gastric mill activity correlates with slowing of
301 the pyloric rhythm [44]. Figure 6C shows LP and PD neurons with rhythmic slow waves.
302 LP and the second PD neuron – seen here on the lvn recording – were bursting. Both
303 neurons became silent due to a strong inhibitory input coinciding with strong LG and
304 MCN1 activity. In Figure 6D, LP and PD neurons were both firing rhythmically.
305 Depolarizing inhibition resulted in tonic firing of LP and no activity on the intracellular
306 recording of PD. In Figure 6E, LP and PD neurons were still bursting. Inhibitory input
307 coincident with LG and MCN1 activity resulted in depolarization of PD and LP and an
308 increased duty cycle of LP bursting.

309 The rhythmic gastric-like activity seen here is similar to gastric mill rhythms
310 elicited upon stimulation of the Ventral Cardiac Neurons (VCNs) [45-47]. Studies have
311 shown that stimulation of VCNs triggers activation of MCN1 and Commissural
312 Projection Neuron 2 (CPN2) in the commissural ganglia (CoGs). This MCN1/CPN2
313 gastric mill rhythm drives the alternation of activity of the protractor motor neurons –
314 LG, GM, MG, and IC – and the retractor motor neurons – DG, VD, and AM. We see
315 similar activity here with strong MCN1 bursts on the ion corresponding to strong LG
316 and GM bursts on the lgn and dgn, respectively, in alternation with DG bursts on the
317 dgn.

318

319 ***The cardiac rhythm is robust to acute changes in pH***

320 To characterize the response of the cardiac rhythm to pH, we bath superfused
321 cardiac preparations with saline between pH 5.9 and pH 11.0 using the same protocol
322 described above for stomatogastric preparations. Figure 7 shows example extracellular
323 recordings from the cardiac ganglia of two animals during the last minute of each pH

324 step. As shown in the top row of CG #1, the ganglion started in control saline at pH 8.2
325 and demonstrated a normal rhythm of small cells and large cells bursting together. As
326 the preparation was subjected to both acidic and basic saline, the rhythm remained. In
327 contrast, the cardiac rhythm in CG #2 became less rhythmic in pH 5.9 and in pH 10.6
328 and above. A normal bursting rhythm recovered after superfusion of control saline as
329 seen in the bottom right box.
330
331 **Fig 7. Robust and variable cardiac rhythm activity across pH.**
332 Two example cardiac ganglion experiments with an acid-first protocol. Each colored box
333 displays 12 seconds of extracellular recordings of the trunk taken from the last minute of
334 each pH condition. Small Cell (SC) and Large Cell (LC) activity is visible. Each
335 experiment can be read left to right then top to bottom in chronological order.
336
337 To characterize these effects, we defined four states of activity: 1) 'SC and LC
338 bursting' rhythm containing both units with a minimum of one LC spike per SC burst; 2)
339 'SC bursting only' rhythm containing only SC bursts with no or inconsistent LC spiking;
340 3) 'all silent'; and 4) 'atypical activity' that could not be categorized under the first three
341 definitions (Fig 8A). Figure 8B shows the mean fraction of time that all preparations
342 spent in these states during the last eight minutes of each pH step. A One-Way
343 Repeated-Measures ANOVA of the effect of pH on the fraction of time the preparations
344 were rhythmic (i.e. SC and LC bursting) revealed a significant effect of both acid
345 ($F(4,56) = 7.462$, $p < 0.0001$) and base ($F(5,70) = 22.495$, $p < 0.0001$) on the cardiac
346 rhythm. Paired samples t-tests confirm that rhythmic activity at pH 5.9 ($t(14) = 3.009$, p

347 = 0.0375), pH 10.1 ($t(14) = 4.593$, $p = 0.0021$), pH 10.6 ($t(14) = 5.805$, $p = 0.0002$), and
348 pH 11.0 ($t(14) = 6.058$, $p = 0.0001$) was significantly different than control pH 8.2.
349
350 **Fig 8. Cardiac rhythm activity characterized by defined states.**
351 (A) Four states were defined to characterize cardiac rhythm activity. Examples of
352 activity for each state are given. (B) Stacked bars give the mean fraction of time that all
353 15 preparations spent in each state over the last eight minutes of each pH step. As pH
354 8.2 was used as a control prior to each ramp and as a recovery after each ramp, four bars
355 for pH 8.2 are shown to maintain the chronology of the protocol; recoveries at pH 8.2
356 are shown on the far left and far right ends of the plot. Asterisks denote statistical
357 significance revealed by paired samples t-tests with Bonferroni correction (* $p < 0.05$; **
358 $p < 0.01$; *** $p < 0.001$).
359
360 To describe these effects quantitatively, mean measures of rhythm frequency, the
361 number of LC spikes per burst, and LC duty cycle were calculated (Fig 9). As shown in
362 Figure 9A, cardiac rhythm frequency declined at extreme pH values. A repeated-
363 measures ANOVA showed a significant effect of both acidic ($F(4,56) = 8.411$, $p <$
364 0.0001) and basic ($F(5,70) = 12.609$, $p < 0.0001$) saline on cardiac rhythm frequency.
365 Paired samples t-tests confirm significantly slower cardiac rhythms at pH 5.9 ($t(14) =$
366 3.156, $p = 0.0280$), pH 6.4 ($t(14) = 3.057$, $p = 0.0341$), pH 10.6 ($t(14) = 3.950$, $p =$
367 0.0073), and pH 11.0 ($t(14) = 3.519$, $p = 0.0170$). Figure 9B displays the mean number of
368 LC spikes per burst as a function of pH. An ANOVA showed significant effects of acid
369 ($F(4,56) = 4.342$, $p = 0.0040$) and base ($F(5,70) = 6.577$, $p < 0.0001$) on LC spikes per
370 burst. The number of LC spikes per burst was significantly different at pH 6.4 ($t(14) =$

371 4.639, $p = 0.0015$) and marginally affected at pH 10.6 ($t(14) = 2.895$, $p = 0.0588$) and
372 pH 11.0 ($t(14) = 2.812$, $p = 0.0693$). Figure 9C reveals a significant effect of base
373 ($F(5,70) = 6.366$, $p < 0.0001$) but not acid ($F(4,56) = 2.058$, $p = 0.0986$) on mean LC
374 duty cycle. Paired samples t-tests confirm significant changes in LC duty cycle at pH
375 10.6 ($t(14) = 3.792$, $p = 0.0099$) and 11.0 ($t(14) = 4.200$, $p = 0.0044$) compared to
376 control.
377
378 **Fig 9. Cardiac rhythm characteristics.**
379 Several characteristics were computed to characterize the cardiac rhythm. Mean data
380 across animals is plotted with vertical lines representing the standard deviation. (A)
381 Mean cardiac rhythm frequency, (B) mean number of LC neuron spikes per burst, and
382 (C) mean LC neuron duty cycle are plotted as a function of pH. As pH 8.2 was used as a
383 control prior to each ramp and as a recovery after each ramp, four values for pH 8.2 are
384 shown to maintain the chronology of the protocol; recoveries at pH 8.2 are shown on the
385 far left and far right ends of the plot on a gray background. Asterisks denote statistical
386 significance revealed by paired samples t-tests with Bonferroni correction (* $p < 0.05$; **
387 $p < 0.01$; *** $p < 0.001$).
388
389 ***The cardiac and pyloric rhythms are differentially sensitive to pH***
390 To compare the effect of pH on the cardiac and pyloric rhythms, the distributions
391 of the fraction of time that each preparation retained a normal rhythm were compared
392 (Fig 10A). A normal rhythm was defined as a triphasic rhythm – a combined metric of
393 states 1 and 2 – and Small Cells and Large Cells bursting together – state 1 – for the
394 pyloric and cardiac rhythms, respectively. A comparison between the rhythmicity of

395 these two ganglia across pH reveals similar distributions with maxima around the
396 control pH of 8.2 and minima at extreme pH values. Interestingly, these distributions
397 appear to be shifted as the CG was more sensitive to extreme base whereas the STG was
398 more sensitive to extreme acid. A Two-Way Mixed-Design ANOVA confirmed significant
399 main effects of pH ($F(4,112) = 7.230$, $p < 0.0001$) and ganglion ($F(1,28) = 9.046$, $p =$
400 0.0055) as well as an interaction between pH and ganglion ($F(4,112) = 5.392$, $p =$
401 0.0005) on rhythmicity in acidic solutions. Similarly, in basic solutions, the fraction of
402 time these ganglia displayed normal rhythms was significantly affected by pH ($F(1,28) =$
403 23.461, $p < 0.0001$), ganglion ($F(5,140) = 8.931$, $p = 0.0058$), and their interaction
404 ($F(5,140) = 3.524$, $p = 0.0050$). Independent samples t-tests with Bonferroni correction
405 confirm differences between the pyloric and cardiac rhythms at pH 5.9 ($t(14) = 3.033$, p
406 $= 0.0226$), 10.1 ($t(14) = 3.052$, $p = 0.0253$), and 10.6 ($t(14) = 3.097$, $p = 0.0222$).
407
408 **Fig 10. Rhythmicity of the cardiac and pyloric rhythms compared across**
409 **pH.**
410 (A) Mean fraction of time that both the pyloric (blue) and cardiac (green) rhythms
411 displayed normal activity is plotted as a function of pH. Differences between the activity
412 of the two rhythms were analyzed by independent samples t-tests at each pH. Asterisks
413 denote statistical significance with Bonferroni correction (* $p < 0.05$; ** $p < 0.01$; *** p
414 < 0.001). (B) Rhythmicity of individual animal preparations is plotted for extreme acid
415 (pH 5.9), control (pH 8.2) and extreme base (pH 11.0) saline conditions. Each column of
416 boxes represents a single preparation, with position across conditions remaining
417 constant. The saturation of each box represents the mean fraction of time with a normal
418 rhythm as indicated by the color bars on the right.

419

420 To understand better the amount of animal-to-animal variability in these two
421 rhythms, the activity of individual preparations was plotted in control pH 8.2, extreme
422 acid pH 5.9, and extreme base pH 11.0 (Fig 10B). Each box represents an individual
423 preparation and its saturation corresponds to the fraction of time with a normal rhythm
424 as defined by the color bars. All preparations were rhythmically bursting at control pH
425 and became less rhythmic in the presence of extreme acid. However, 14 of 15 STG
426 preparations ceased firing after 15 minutes of exposure to pH 5.9. In contrast, only 6 of
427 15 CG preparations showed reductions in rhythmic activity at pH 5.9. Three of the 15 CG
428 preparations maintained a normal rhythm in every pH condition. Interestingly, STG
429 preparations that showed decrements in activity during basic conditions were extremely
430 susceptible to reductions in activity during extreme acid. The opposite is true in CG
431 preparations suggesting that activity in base is a better predictor of acid activity in the
432 STG and vice versa in the CG. This finding also suggests that some preparations were
433 more susceptible to the effects of pH than others.

434 **Discussion**

435 Circuit dynamics depend on the properties of the constituent neurons and their
436 synaptic connections. Likewise, the intrinsic excitability of an individual neuron
437 depends on the relative quantity and function of its voltage- and time-dependent
438 channels. Given that the physiological properties of ion channels are known to be
439 sensitive to pH [22-24, 48-58], one might imagine that a neuronal circuit is as sensitive
440 to changes in pH as its most sensitive ion channels. Therefore, it is surprising that both
441 the pyloric rhythm of the STG and the cardiac ganglion rhythm in the crab, *C. borealis*,
442 are relatively insensitive to acute pH change from about pH 6.4 to pH 9.6 when the
443 individual functions of many ion channels are considerably altered within this pH range.

444 pH is carefully regulated in most vertebrate animals. Slight acidosis or alkalosis
445 can have deleterious effects on many aspects of vertebrate physiology [59], which may
446 be partially a consequence of the relative sensitivity of many vertebrate ion channels and
447 synapses to pH. Unfortunately, little is known about the pH sensitivity of crustacean ion
448 channels, but it would be surprising if it differed drastically from that seen in
449 vertebrates as there is considerable homology across phylogeny in channel structure and
450 function. However, it is possible that modest evolutionary changes in channel structure
451 occurred to allow endothermic animals to function in high temperature and low pH
452 conditions.

453 Crab central pattern generating circuits are robust and adaptable to a large range
454 of temperatures [60-63]. This circuit robustness might be a result of a relative
455 insensitivity of the ion channel conductance densities and rate constants that underlie
456 network behavior. Computational models of neurons and small networks such as the
457 pyloric rhythm show numerous, degenerate solutions [34, 64-70], which may allow

458 these networks to withstand relatively large changes in effective channel function.
459 Indeed, many models show little effect on network performance of two-fold changes in
460 effective channel densities or 30 to 40 percent changes in activation and inactivation
461 rates. Therefore, one prediction of the relative pH insensitivity of these networks is that
462 numerous pH sensitive changes occur across the population of ion channels, but that
463 these circuits have evolved sets of correlated ion channels that compensate for these
464 changes [69, 71-75].

465 In addition to the relative pH insensitivity of these circuits, we were surprised
466 that the cardiac and pyloric rhythms of *C. borealis* are differentially sensitive to acid and
467 base. This was unexpected as many of the same ion channels are found in the two
468 ganglia [70, 75-79]. One possible explanation of this intriguing finding is that the burst
469 generating mechanisms in the two networks may be substantially different. For
470 example, the pyloric rhythm depends heavily on post-inhibitory rebound as a timing
471 mechanism [80-82] while the cardiac ganglion depends on strong excitatory drive from
472 the pacemaker neurons [83]. One simple possibility is that the excitatory and inhibitory
473 synaptic connections are differentially sensitive to pH. Additionally, although both
474 networks are driven by bursting pacemaker neurons, the contribution of different ion
475 channels to the burst generating mechanism may be sufficiently different in the two
476 cases such that the pacemakers themselves respond differently to high and low pH.

477 Further, we found that the membrane potential of the isolated pyloric neurons,
478 LP and PD, varied differentially with changing extracellular pH. Isolated LP neurons
479 fired tonically and depolarized in extreme base while isolated PD neurons depolarized in
480 acid. We observed depolarization in acid for both neurons in intact preparations,
481 suggesting an important role of synaptic input in regulating activity across pH.

482 Together, these results illustrate the potential difficulty in generalizing the effects of
483 environmental perturbation across neurons and circuits, even within the same animal.
484 Additionally, we found that under most control conditions, the gastric mill
485 rhythm was silent. Unexpectedly, gastric mill rhythms were frequently activated upon
486 exposure to or recovery from extreme pH. It is possible that either sensory or
487 modulatory axons were activated by the pH changes, and it is feasible that sensory
488 and/or modulatory neurons might be normally part of a response to altered pH.
489 In this study, we examined the effects of manipulating extracellular pH; however,
490 the extent to which intracellular pH was affected and its contribution to changes in
491 activity remain unclear. We did observe that neurons penetrated with intracellular
492 recording electrodes exhibited more labile activity in response to changing pH. This may
493 indicate that changes in intracellular pH would be more deleterious than what occurs in
494 response to changes in extracellular pH alone.
495 The ocean environment is both warming and acidifying at historic rates. *Cancer*
496 *borealis* maintains relatively robust pyloric and cardiac rhythms in the temperature
497 ranges it usually experiences, from 3°C to 25°C [84-87]. Importantly, the effect of
498 temperature on ocean pH is relatively modest in comparison to the range of pH studied
499 here. In *Carcinus meanus*, exposure to artificial ocean acidification produced relatively
500 small changes in hemolymph pH [88]. Therefore, unlike some ocean organisms that are
501 very sensitive to even small ocean pH changes, we predict that the neuronal circuits in
502 *C. borealis*, at least as an adult, will be largely insensitive to changes in ocean pH.
503 However, other physiological parameters, such as metabolic rates and hemolymph flow
504 may be more pH sensitive [88]. Moreover, network performance may be further

505 attenuated when pH is coupled to increasing temperature and other environmental
506 insults.

507 Previous research revealed robust activity and increasing frequency of the pyloric
508 rhythm of the STG and cardiac rhythm of the CG in response to increasing temperature
509 in both *in vivo* and *ex vivo* preparations [35-37]. Contrastingly, increasing pH reveals
510 non-linear effects on activity.

511 The data in this paper and in our previous work on temperature reveal
512 considerable animal-to-animal variability in response to extreme perturbations. Here,
513 all animals behaved predictably and reliably across more than a thousand-fold change in
514 hydrogen ion concentration, an unexpectedly large range of robust performance. At
515 more extreme pH, animal-to-animal variably became apparent, consistent with the
516 response of these circuits to extreme temperatures [84-87]. This animal-to-animal
517 variability is almost certainly a consequence of the fact that similar network
518 performance can arise from quite variable sets of underlying conductances [64, 89-91].
519 What remains to be seen is whether animals that are more robust to a given extreme
520 perturbation are less robust to others and whether there are given sets of network
521 parameters that confer robustness to many different perturbations.

522 **Materials and Methods**

523 ***Animals***

524 From March 2016 to May 2018, adult male Jonah crabs (*Cancer borealis)*
525 weighing between 400 and 700 grams were obtained from Commercial Lobster (Boston,
526 MA). Before experimentation, all animals were housed in tanks with flowing artificial
527 seawater (Instant Ocean) between 10°C and 13°C on a 12-hour light/dark cycle without
528 food. Animals were kept in tanks for a maximum of two weeks. Animals were removed
529 from tanks and kept on ice for 30 minutes prior to dissection.

530

531 ***Saline Solutions***

532 Control *C. borealis* physiological saline was composed of 440 mM NaCl, 11 mM
533 KCl, 13 mM $CaCl_2$, 26 mM $MgCl_2$, 11 mM Trizma base, and 5 mM Maleic acid. Additional
534 quantities of concentrated HCl and NaOH were added to achieve solutions with pH 5.5,
535 6.0, 6.5, 7.0, 7.5, 8.0, 8.5, 9.0, 9.5, and 10.0 at room temperature (~23°C). Solution pH
536 was measured again at 11°C to be 5.9, 6.4, 7.0, 7.6, 8.2, 9.0, 9.6, 10.1, 10.6, and 11.0,
537 respectively. Solution pH was measured using a calibrated pH/ion meter (Mettler
538 Toledo S220). For experiments with picrotoxin, 10^{-5} M PTX was added to each of the pH
539 solutions.

540

541 ***Electrophysiology***

542 The stomatogastric and cardiac nervous systems were dissected out of the
543 animals and pinned out in a Sylgard (Dow Corning) coated plastic Petri dish containing
544 chilled saline (11°C). In all cases, we worked only with fully intact stomatogastric

545 nervous system preparations that included the commissural and esophageal ganglia and
546 their descending nerves. Only preparations containing healthy rhythms with no sign of
547 damage from dissection were analyzed.

548 Vaseline wells were placed around motor nerves and extracellular recordings
549 were obtained using stainless steel pin electrodes placed in the wells and amplified using
550 a differential amplifier (A-M Systems Model 1700). Intracellular sharp-electrode
551 recordings were obtained from cell bodies in the stomatogastric ganglion using a
552 microelectrode amplifier (Molecular Devices Axoclamp 2B or 900A) with HS-2A-x1LU
553 headstages holding 15-30 MΩ boroscilate microelectrodes with filaments (Sutter
554 Instrument Co. BF150-86-10) pulled with a Flaming/Brown micropipette puller (Sutter
555 Instrument Co. P-97). Microelectrodes were filled with a solution of 10 mM $MgCl_2$, 400
556 mM potassium gluconate, 10 mM HEPES, 15 mM Na_2SO_4, and 20 mM NaCl [92].

557 Preparations were continuously superfused with physiological saline at 11°C.
558 Superfusion was gravity fed at approximately nine mL/min. The temperature of the
559 superfusing saline was controlled and recorded using a Peltier device (Warner
560 Instruments CL-100). Instantaneous bath pH was recorded using a pH microelectrode
561 placed adjacent to the ganglion (Thermo Scientific Orion 9810BN) combined with a
562 preamplifier (Omega PHTX-21). Output from the pH microelectrode was converted
563 from arbitrary voltage to pH using a temperature-compensated calibration.

564

565 ***Data Acquisition and Analysis***

566 Data were acquired using a data acquisition board (Molecular Devices Digidata
567 1440A) and Clampex 10.5 software (Molecular Devices). Data were analyzed using

568 Clampfit 10.5, Spike2 v 6.04 (Cambridge Electronic Design), and/or MATLAB 2017A
569 (MathWorks).
570 For Figures 3, 4, 8, 9, and 10, we analyzed the last eight minutes of extracellular
571 recordings of the lvn of the STG or the trunk of the CG for each 15-minute pH step to
572 ensure that preparations had reached a steady state.
573 For Figures 3, 8, and 10, data were categorized into states. A transition from one
574 state to another was noted when there was a sustained change in activity from one state
575 to another lasting a minimum of 10 seconds, corresponding to approximately 10 pyloric
576 cycles and 3 cardiac cycles of rhythmic activity. In other words, if the rhythm
577 transitioned from one state into another and maintained the new state of activity for at
578 least 10 seconds, a transition was noted at the start of that new state. Rhythms rarely
579 transitioned intermittently between two states (e.g. once a rhythm had transitioned
580 from normal triphasic to weak triphasic, it rarely transitioned back to normal triphasic
581 until after recovery in control pH). Further, rhythms generally transitioned in a
582 stereotypical pattern. For STG preparations, the pyloric rhythm often transitioned from
583 normal triphasic to weak triphasic to intermittent triphasic to all silent. For CG
584 preparations, the cardiac rhythm usually transitioned from SC and LC bursting to SC
585 bursting only to all silent. During recovery, these transition patterns were reversed. The
586 mean fraction of time that the preparations remained in each state during the last eight
587 minutes of recording at each pH step is plotted.
588 For Figures 4 and 9, quantitative variables of mean frequency, mean number of
589 spikes per burst, and mean duty cycle were measured. Spikes and bursts were first
590 isolated in Spike2 by thresholding extracellular recordings. MATLAB was then used for
591 further analysis. Mean burst frequency was calculated by finding the total number of

592 bursts in the last eight minutes of each pH condition and dividing by the total number of
593 seconds. The mean number of spikes per burst of a given neuron reflects the mean of the
594 number of spikes contributing to each burst. Duty cycle was calculated by finding the
595 mean of the burst duration divided by the length of the cycle as measured from the start
596 of the burst to the beginning of the next burst.

597 For Figure 5, the last minute of each pH step was analyzed in MATLAB for
598 intracellular recordings of isolated LP and PD neurons. Minimum membrane potential
599 was calculated by finding the mean of the minimum voltage of the neuron between each
600 burst. Recordings were then low-pass filtered to remove spikes from the slow wave.
601 Mean slow wave amplitude was measured by averaging the difference between troughs
602 and peaks of the slow wave's membrane potential. Spike amplitude was retrieved by
603 subtracting the filtered slow wave signal from the original recording and then measuring
604 the mean amplitude from trough to peak of each action potential. PD burst frequency
605 was calculated by finding the mean inverse of the time period between one slow wave
606 trough to the next. LP firing rate was determined by calculating the mean of the inverse
607 of the inter-spike interval, the time between spikes.

608

609 ***Statistics***

610 All statistics were performed using R (version 3.4.3). For Figures 3, 4, 5, 8, and 9,
611 we performed statistical testing using a Univariate Type III Repeated-Measures Analysis
612 of Variance (ANOVA) from the car package. Separate tests were performed for acid and
613 base step protocols. Post-hoc paired sample t-tests with Bonferroni correction were
614 performed for each pH step against its respective control. For Figure 10, we performed
615 Two-Way Mixed-Samples ANOVA (Type III) for both acid and base step protocols using

616 the car package. Post-hoc independent samples t-tests with Bonferroni correction were

617 performed for each pH condition.

References

1. Donahue MJ, Nichols A, Santamaria CA, League-Pike PE, Krediet CJ. Predation risk, prey abundance, and the vertical distribution of three brachyuran crabs on Gulf of Maine shores. J Crust Biol. 2009;29:523–31.
2. Haeffner Jr PA. Aspects of the biology of the Jonah crab, *Cancer borealis* Stimpson, 1859 in the mid Atlantic Bight. J Nat Hist. 1977;11:303–20.
3. Stehlik LL, MacKenzie CL, Morse WW. Distribution and abundance of four brachyuran crabs on the northwest Atlantic shelf. Fish Bull. 1991;89:473–92.
4. Macfarling MC, Etheridge D, Trudinger C, Steele P, Lagenfelds R, Van Ommen T, et al. Law Dome CO_2, CH_4 and N_2O ice core records extended to 2000 years BP. Geophys Res Lett. 2006;33(14).
5. Buchel C, Coull JT, Friston KJ. The predictive value of changes in effective connectivity for human learning. Science. 1999;283(5407):1538-41.
6. Canadell JG, Le Quéré C, Raupach MR, Field CB, Buitenhuis ET, Ciais P, et al. Contributions to accelerating atmospheric CO_2 growth from economic activity, carbon intensity, and efficiency of natural sinks. Proc Natl Acad Sci USA. 2007;104(47):18866-70.
7. Knorr W. Is the airborne fraction of anthropogenic CO_2 emissions increasing? Geophys Res Lett. 2009;36(21).
8. Wittman AC, Pörtner HO. Sensitivities of extant animal taxa to ocean acidification. Nat Clim Change. 2013;3(11):995.
9. Kelly MW, Hofmann GE. Adaptation and the physiology of ocean acidification. Funct Ecol. 2013;27(4):980-90.
10. Webb SJ, Tu J, Cory E, Morgan V, Sah R, Deheyn DD, et al. Stress physiology and weapon integrity of intertidal mantis shrimp under future ocean conditions. Sci Rep. 2016;6:38637.
11. Dove ADM, Allam B, Powers JJ, Sokolowski MS. A Prolonged thermal stress experiment on the american lobster, *Homarus americanus*. J Shellfish Res. 2005;24(3):761-5.
12. Pearce J, Balcom N. The 1999 Long Island Sound lobster mortality event: Findings of the comprehensive research initiative. J Shellfish Res. 2005;24(3):133-9.
13. Qadri SA, Camacho J, Wang H, Taylor JR, Grosell M, Worden MK. Temperature and acid–base balance in the American lobster *Homarus americanus*. J Exp Biol. 2007;210(7):1245-54.
14. Truchot J-P. Mechanisms of extracellular acid-base regulation as temperature changes in decapod crustaceans. Respir Physiol. 1973;33:161-76.
15. Howell BJ, Rahn H, Goodfellow D, Herreid C. Acid-base regulation and temperature in selected invertebrates as a function of temperature. Am Zool. 1973;13(2):557-63.
16. Truchot J-P. Changes in the hemolymph acid-base state of the shore crab, *Carcinus maenas*, exposed to simulated tidepool conditions. Biol Bull. 1986;170(3):506-18.
17. Vogt KE, Regehr WG. Cholinergic modulation of excitatory synaptic transmission in the CA3 area of the hippocampus. J Neurosci. 2001;21(1):75-83.

18. Somero GN. pH-temperature interactions on proteins: Principles of optimal pH and buffer system design. Mar Biol Lett. 1981;2:163-78.
19. Reeves RB. An imidazole alphastat hypothesis for vertebrate acid-base regulation: Tissue carbon dioxide content and body temperature in bullfrogs. Respir Physiol. 1972;14(1):219-36.
20. Reeves RB. The interaction of body temperature and acid-base balance in ectothermic vertebrates. Annu Rev Physiol. 1977;39(1):559-86.
21. Truchot J-P. Temperature and acid-base regulation in the shore crab Carcinus maenas (L.). Respir Physiol. 2003;17(1):11-20.
22. Doering CJ, McRory JE. Effects of extracellular pH on neuronal calcium channel activation. Neuroscience. 2007;146(3):1032-43.
23. Hille B. Charges and potentials at the nerve surface: divalent ions and pH. J Gen Physiol. 1968;51(2):221-36.
24. Tombaugh GC, Somjen GG. Effects of extracellular pH on voltage-gated Na^+, K^+ and Ca^{2+} currents in isolated rat CA1 neurons. J Physiol. 1996;493(3):719-32.
25. Zhou W, Jones SW. The effects of external pH on calcium channel currents in bullfrog sympathetic neurons. Biophys J. 1996;70(3):1326-34.
26. Mozhaev GA, Mozhaeva GN, Naumov AP. Effect of calcium ions on the steady-state potassium conductivity of the Ranvier node membrane. Tsitologiia. 1970;12(8):993-1001.
27. Wanke E, Carbone E, Testa PL. K^+ conductance modified by a titratable group accessible to protons from the intracellular side of the squid axon membrane. Biophys J. 1979;26(2):319-24.
28. Woodhull AM. Ionic blockage of sodium channels in nerve. J Gen Physiol. 1973;61(6):687-708.
29. Courtney KR. Extracellular pH selectively modulates recovery from sodium inactivation in frog myelinated nerve. Biophys J. 1979;28(2):363-8.
30. Billups B, Atwell D. Modulation of non-vesicular glutamate release by pH. Nature. 1996;379(6561):171.
31. Bloch W, Addicks K, Hescheler J, Fleischmann BK. Nitric oxide synthase expression and function in embryonic and adult cardiomyocytes. Microsc Res Tech. 2001;55(4):259-69.
32. Sinning A, Liebmann L, Kougioumtzes A, Westermann M, Bruehl C, Hübner CA. Synaptic glutamate release is modulated by the Na^+-driven Cl^-/HCO_3^- exchanger Slc4a8. J Neurosci. 2011;31(20):7300-11.
33. Sinning A, Hübner CA. Minireview: pH and synaptic transmission. FEBS Lett. 2013;587(13):1923-8.
34. Goldman MS, Golowasch J, Marder E, Abbott LF. Global structure, robustness, and modulation of neuronal models. J Neurosci. 2001;21(14):5229-38.
35. Marder E, Tang LS. Coordinating different homeostatic processes. Neuron. 2010;66(2):161-3.
36. Delogu A, Sellers K, Zagoraiou L, Bocianowska-Zbrog A, Mandal S, Guimera J, et al. Subcortical visual shell nuclei targeted by ipRGCs develop from a Sox14+-GABAergic progenitor and require Sox14 to regulate daily activity rhythms. Neuron. 2012;75(4):648-62.
37. Kushinsky D, Marder E. In vivo effects of temperature on the heart and pyloric rhythms in the crab, Cancer borealis. bioRxiv. 2018:249631.

38. Beltz B, Eisen JS, Flamm R, Harris-Warrick RM, Hooper SL, Marder E. Serotonergic innervation and modulation of the stomatogastric ganglion of three decapod crustaceans (*Panulirus interruptus, Homarus americanus* and *Cancer irroratus*). J Exp Biol. 1984;109:35-54.
39. Marder E, Bucher D. Understanding circuit dynamics using the stomatogastric nervous system of lobsters and crabs. Annu Rev Physiol. 2007;69:291-316.
40. Nusbaum MP, Blitz DM, Marder E. Functional consequences of neuropeptide and small-molecule co-transmission. Nat Rev Neurosci. 2017;18(7):389-403.
41. Mulloney B, Selverston AI. Organization of the stomatogastric ganglion in the spiny lobster. I. Neurons driving the lateral teeth. J Comp Physiol. 1974;91:1-32.
42. Mulloney B, Selverston AI. Organization of the stomatogastric ganglion in the spiny lobster. III. Coordination of the two subsets of the gastric system. J Comp Physiol. 1974;91:53-78.
43. Blitz DM, Christie AE, Coleman MJ, Norris BJ, Marder E, Nusbaum MP. Different proctolin neurons elicit distinct motor patterns from a multifunctional neuronal network. J Neurosci. 1999;19:5449-63.
44. Bucher D, Johnson CD, Marder E. Neuronal morphology and neuropil structure in the stomatogastric ganglion of the lobster, *Homarus americanus*. J Comp Neurol. 2007;501(2):185-205.
45. White RS, Nusbaum MP. The same core rhythm generator underlies different rhythmic motor patterns. J Neurosci. 2011;31(32):11484-94.
46. Beenhakker MP, Kirby MS, Nusbaum MP. Mechanosensory gating of proprioceptor input to modulatory projection neurons. J Neurosci. 2007;27(52):14308-16.
47. Saideman SR, Blitz DM, Nusbaum MP. Convergent motor patterns from divergent circuits. J Neurosci. 2007;27(25):6664-74.
48. Catterall WA. From ionic currents to molecular mechanisms: the structure and function of voltage-gated sodium channels. Neuron. 2000;26(1):13-25.
49. Mahapatra S, Marcanoti A, Vandael DH, Striessnig J, Carbone E. Are Cav1.3 pacemaker channels in chromaffin cells? Possible bias from resting cell conditions and DHP blockers usage: Possible bias from resting cell conditions and DHP blocker usage. Channels. 2011;5(3):219-24.
50. Marcanoti A, Vandael DH, Mahapatra S, Carabelli V, Sinnegger-Brauns MJ, Striessnig J, et al. Loss of Cav1.3 channels reveals the critical role of L-type and BK channel coupling in pacemaking mouse adrenal chromaffin cells. J Neurosci. 2010;30(2):219-24.
51. Cens T, Rousset M, Charnet P. Two sets of amino acids of the domain I of Cav2.3 Ca(2+) channels contribute to their high sensitivity to extracellular protons. Pfluegers Arch/Eur J Physiol. 2011;462:303-14.
52. Anwar H, Li X, Bucher D, Nadim F. Functional roles of short-term synaptic plasticity with an emphasis on inhibition. Curr Opin Neurobiol. 2017;43:71-8.
53. Harms E, Stoetzer C, Stueber T, O'Reilly AO, Leffler A. Investigation into the role of an extracellular loop in mediating proton-evoked inhibition of voltage-gated sodium channels. Neurosci Lett. 2017;661:5-10.
54. Vilin YY, Peters CH, Ruben P. Acidosis differentially modulates inactivation in $Na_v1.2$, $Na_v1.4$, and $Na_v1.5$ channels. Front Pharmacol. 2012;3:109.

55. Zhou Y, Xia X, Lingle CJ. BK channel inhibition by strong extracellular acidification. bioRxiv. 2018:317339.
56. Cook DL, Ikeuchi M, Fujimoto W. Lowering of pH_i inhibits Ca^{2+}-activated K^+ channels in pancreatic B-cells. Nature. 1984;31:269-71.
57. Bayliss DA, Barhanin J, Gestrau C, Guyenet PG. The role of pH-sensitive TASK channels in central respiratory chemoreception. Pfluegers Arch/Eur J Physiol. 2015;467(5):917-29.
58. Guarina L, Vandael DH, Carabelli V, Carbone E. Low pH_o boosts burst firing and catecholamine release by blocking TASK-1 and BK channels while preserving Cav1 channels in mouse chromaffin cells. J Physiol. 2017;595(8):2587-609.
59. Chesler M. Regulation and modulation of pH in the brain. Physiol Rev. 2003;83(4):1183-221.
60. DFO. Can Sci Advis Sec Sci Advi Rep**2009**.
61. Haddad SA, Marder E. Circuit robustness to temperature perturbation is altered by neuromodulators. bioRxiv. 2017:178764.
62. Tang LS, Goeritz ML, Caplan JS, Taylor AL, Fisek M, Marder E. Precise temperature compensation of phase in a rhythmic motor pattern. PLoS Biol. 2010;8(8).
63. Tang LS, Taylor AL, Rinberg A, Marder E. Robustness of a rhythmic circuit to short and long-term temperature changes. J Neurosci. 2012;32(29):10075-85.
64. Prinz AA, Bucher D, Marder E. Similar network activity from disparate circuit parameters. Nat Neurosci. 2004;7(12):1345-52.
65. Golowasch J, Casey M, Abbott LF, Marder E. Network stability from activity-dependent regulation of neuronal conductances. Neural Comput. 1999;11(5):1079-96.
66. Golowasch J, Goldman MS, Abbott LF, Marder E. Failure of averaging in the construction of a conductance-based neuron model. J Neurophysiol. 2002;87(2):1129-31.
67. Gutierrez GJ, Marder E. Modulation of a single neuron has state-dependent actions on circuit dynamics. eNeuro. 2014;1(1).
68. Gutierrez GJ, O'Leary T, Marder E. Multiple mechanisms switch an electrically coupled, synaptically inhibited neuron between competing rhythmic oscillators. Neuron. 2013;77(5):845-58.
69. O'Leary T, Williams AH, Franci A, Marder E. Cell types, network homeostasis, and pathological compensation from a biologically plausible ion channel expression model. Neuron. 2014;82(4):809-21.
70. Ransdell JL, Nair SS, Schulz DJ. Neurons within the Same Network Independently Achieve Conserved Output by Differentially Balancing Variable Conductance Magnitudes. Journal of Neuroscience. 2013;33(24):9950-6.
71. O'Leary T, Marder E. Temperature-robust neural function from activity-dependent ion channel regulation. Current Biology. 2016;26(21):2935-41.
72. O'Leary T, Williams AH, Caplan JS, Marder E. Correlations in ion channel expression emerge from homeostatic tuning rules. Proc Natl Acad Sci U S A. 2013;110(28):E2645-54.
73. Temporal S, Desai M, Khorkova O, Varghese G, Dai A, Schulz DJ, et al. Neuromodulation independently determines correlated channel expression and

conductance levels in motor neurons of the stomatogastric ganglion. J Neurophysiol. 2012;107(2):718-27.
74. Temporal S, Lett KM, Schulz DJ. Activity-dependent feedback regulates correlated ion channel mRNA levels in single identified motor neurons. Curr Biol. 2014;24(16):1899-904.
75. Tobin AE, Cruz-Bermudez ND, Marder E, Schulz DJ. Correlations in ion channel mRNA in rhythmically active neurons. PLoS ONE. 2009;4(8):e6742.
76. Schulz DJ, Goaillard JM, Marder E. Variable channel expression in identified single and electrically coupled neurons in different animals. Nat Neurosci. 2006;9:356 - 62.
77. Schulz DJ, Goaillard JM, Marder EE. Quantitative expression profiling of identified neurons reveals cell-specific constraints on highly variable levels of gene expression. Proc Natl Acad Sci U S A. 2007;104(32):13187-91.
78. Northcutt AJ, Lett KM, Garcia VB, Diester CM, Lane BJ, Marder E, et al. Deep sequencing of transcriptomes from the nervous systems of two decapod crustaceans to characterize genes important for neural circuit function and modulation. BMC genomics. 2016;17.
79. Ransdell JL, Temporal S, West NL, Leyrer ML, Schulz DJ. Characterization of inward currents and channels underlying burst activity in motoneurons of crab cardiac ganglion. Journal of Neurophysiology. 2013;110(1):42-54.
80. Hartline DK, Gassie DV, Jr. Pattern generation in the lobster (*Panulirus*) stomatogastric ganglion. I. Pyloric neuron kinetics and synaptic interactions. Biol Cybern. 1979;33(4):209-22.
81. Harris-Warrick RM, Coniglio LM, Barazangi N, Guckenheimer J, Gueron S. Dopamine modulation of transient potassium current evokes phase shifts in a central pattern generator network. J Neurosci. 1995;15:342-58.
82. Harris-Warrick RM, Coniglio LM, Levini RM, Gueron S, Guckenheimer J. Dopamine modulation of two subthreshold currents produces phase shifts in activity of an identified motoneuron. J Neurophysiol. 1995;74(4):1404-20.
83. Cooke IM. Studies on the crustacean cardiac ganglion. Comp Biochem Physiol C. 1988;91(1):205-18.
84. Soofi W, Goeritz ML, Kispersky TJ, Prinz AA, Marder E, Stein W. Phase maintenance in a rhythmic motor pattern during temperature changes *in vivo*. J Neurophysiol. 2014;111(12):2603-13.
85. Tang LS, Goeritz ML, Caplan JS, Taylor AL, Fisek M, Marder E. Precise temperature compensation of phase in a rhythmic motor pattern. PLoS Biol. 2010;8(8):e1000469.
86. Tang LS, Taylor AL, Rinberg A, Marder E. Robustness of a rhythmic circuit to short- and long-term temperature changes. J Neurosci. 2012;32(29):10075-85.
87. Marder E, Haddad SA, Goeritz ML, Rosenbaum P, Kispersky T. How can motor systems retain performance over a wide temperature range? Lessons from the crustacean stomatogastric nervous system. J Comp Physiol A Neuroethol Sens Neural Behav Physiol. 2015;201(9):851-6.
88. Maus B, Bock C, Portner HO. Water bicarbonate modulates the response of the shore crab Carcinus maenas to ocean acidification. J Comp Physiol B. 2018.

89. Goaillard JM, Taylor AL, Schulz DJ, Marder E. Functional consequences of animal-to-animal variation in circuit parameters. Nat Neurosci. 2009;12(11):1424-30.
90. Grashow R, Brookings T, Marder E. Reliable neuromodulation from circuits with variable underlying structure. Proc Natl Acad Sci U S A. 2009;106(28):11742-6.
91. Grashow R, Brookings T, Marder E. Compensation for variable intrinsic neuronal excitability by circuit-synaptic interactions. J Neurosci. 2010;30(27):9145-56.
92. Hooper SL, Thuma JB, Guschlbauer C, Schmidt J, Buschges A. Cell dialysis by sharp electrodes can cause nonphysiological changes in neuron properties. J Neurophysiol. 2015;114(2):1255-71.

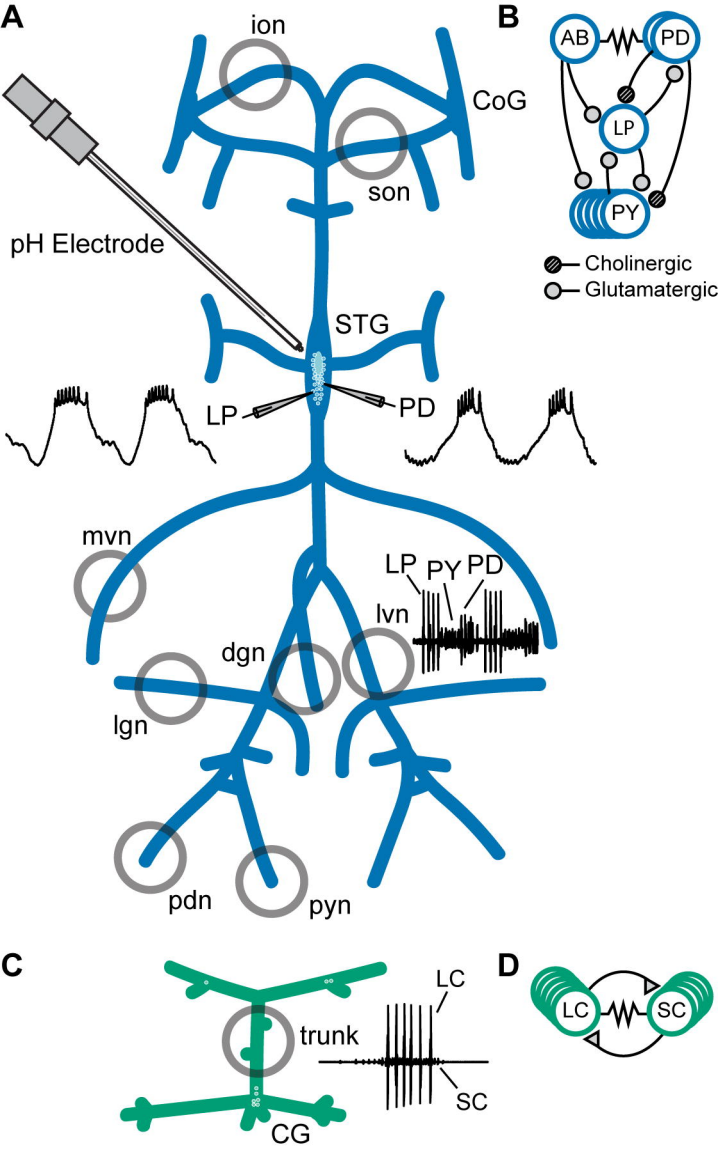
A
ion
CoG
son
pH Electrode
STG
LP
PD
mvn
LP
PY
PD
lvn
dgn
lgn
pdn
pyn
B
AB
PD
LP
PY
Cholinergic
Glutamatergic
C
trunk
LC
SC
CG
D
LC
SC

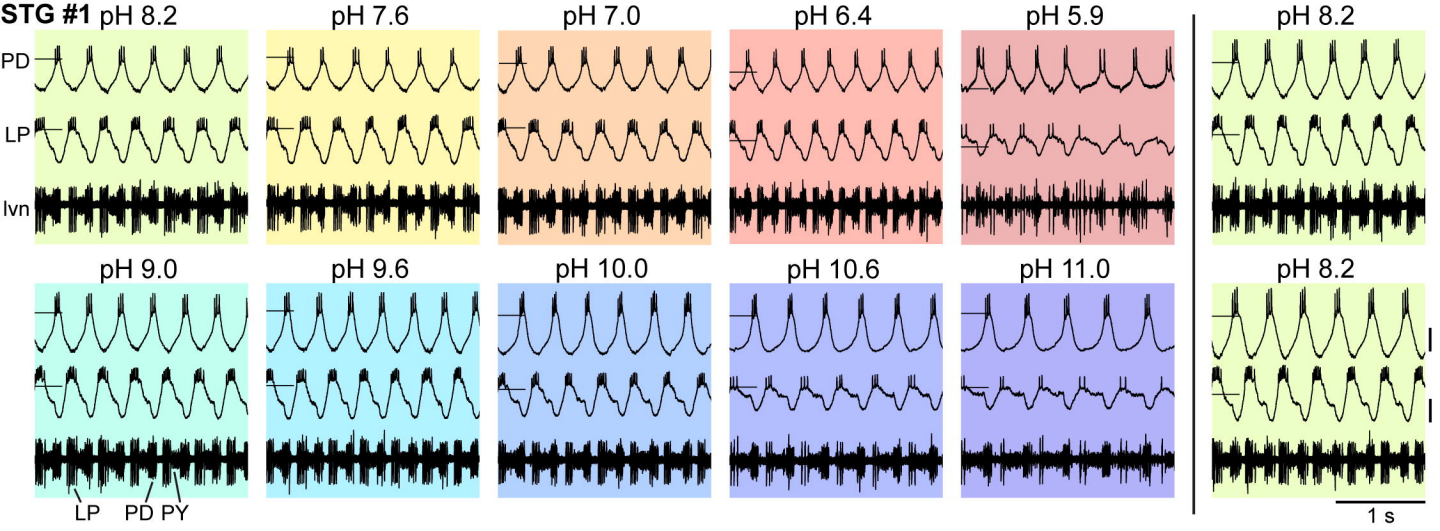
STG #1
pH 8.2
pH 7.6
pH 7.0
pH 6.4
pH 5.9
pH 8.2
PD
LP
lvn
pH 9.0
pH 9.6
pH 10.0
pH 10.6
pH 11.0
pH 8.2
LP
PD
PY
1 s

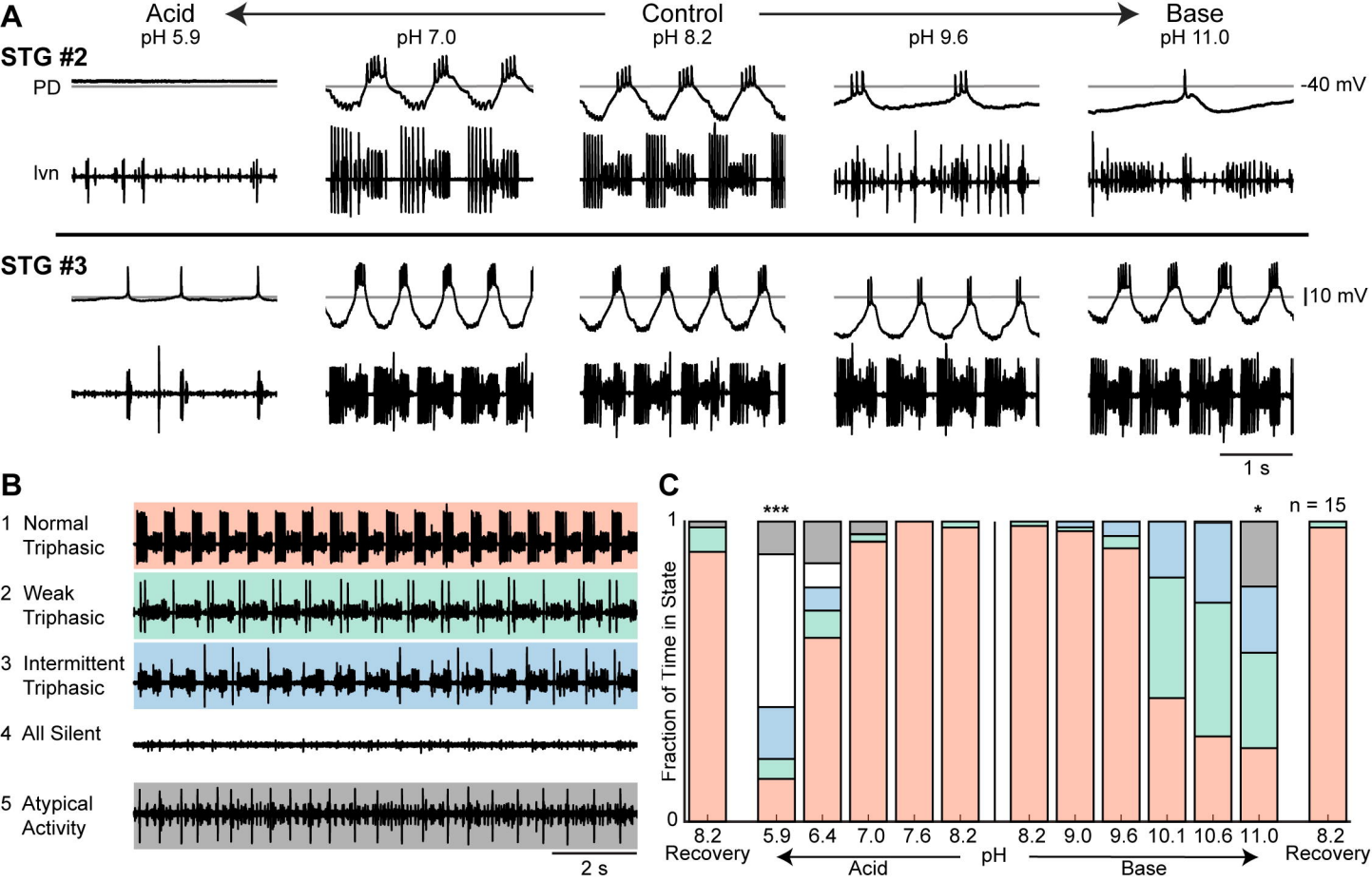
A
Acid
pH 5.9
Control
pH 8.2
Base
pH 7.0
pH 9.6
pH 11.0
STG #2
PD
lvn
-40 mV
STG #3
10 mV
1 s
B
1 Normal Triphasic
2 Weak Triphasic
3 Intermittent Triphasic
4 All Silent
5 Atypical Activity
2 s
C
n = 15
***
*
Fraction of Time in State
1
0
8.2 Recovery
5.9
6.4
7.0
7.6
8.2
8.2
9.0
9.6
10.1
10.6
11.0
8.2 Recovery
Acid
pH
Base

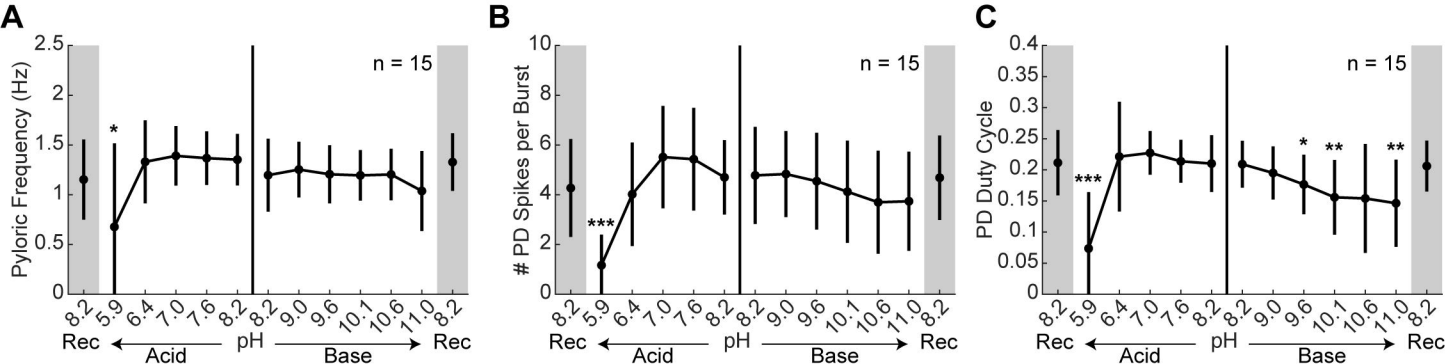
A
Pyloric Frequency (Hz)
n = 15
*
8.2 5.9 6.4 7.0 7.6 8.2 8.2 9.0 9.6 10.1 10.6 11.0 8.2
Rec Acid pH Base Rec
B
# PD Spikes per Burst
n = 15
***
8.2 5.9 6.4 7.0 7.6 8.2 8.2 9.0 9.6 10.1 10.6 11.0 8.2
Rec Acid pH Base Rec
C
PD Duty Cycle
n = 15
***
*
**
**
8.2 5.9 6.4 7.0 7.6 8.2 8.2 9.0 9.6 10.1 10.6 11.0 8.2
Rec Acid pH Base Rec

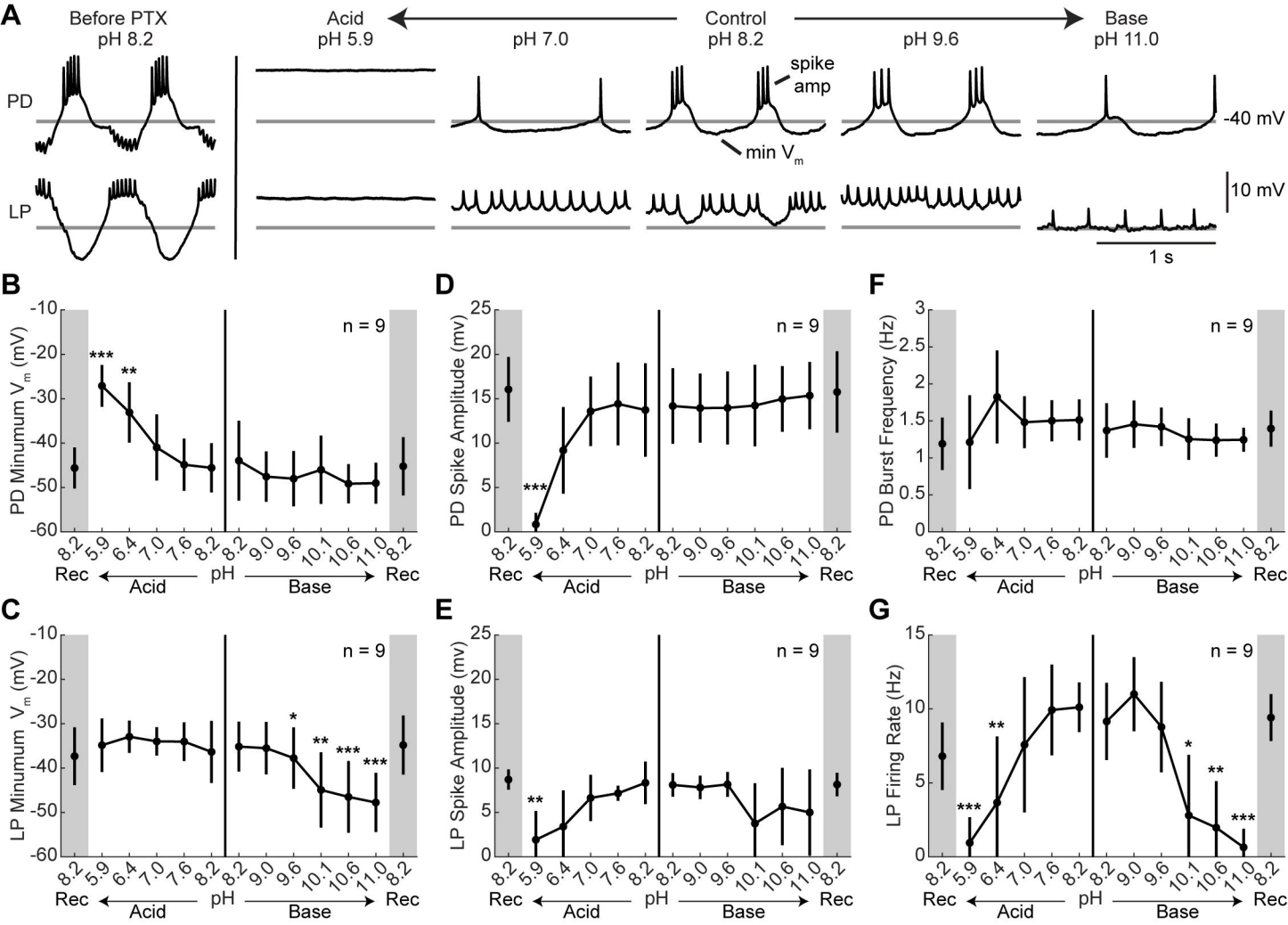
A
Before PTX
pH 8.2
Acid
pH 5.9
pH 7.0
Control
pH 8.2
pH 9.6
Base
pH 11.0
PD
LP
spike
amp
min V_m
-40 mV
10 mV
1 s
B
PD Minumum V_m (mV)
n = 9
C
LP Minumum V_m (mV)
n = 9
D
PD Spike Amplitude (mv)
n = 9
E
LP Spike Amplitude (mv)
n = 9
F
PD Burst Frequency (Hz)
n = 9
G
LP Firing Rate (Hz)
n = 9
Rec
Acid
pH
Base
Rec

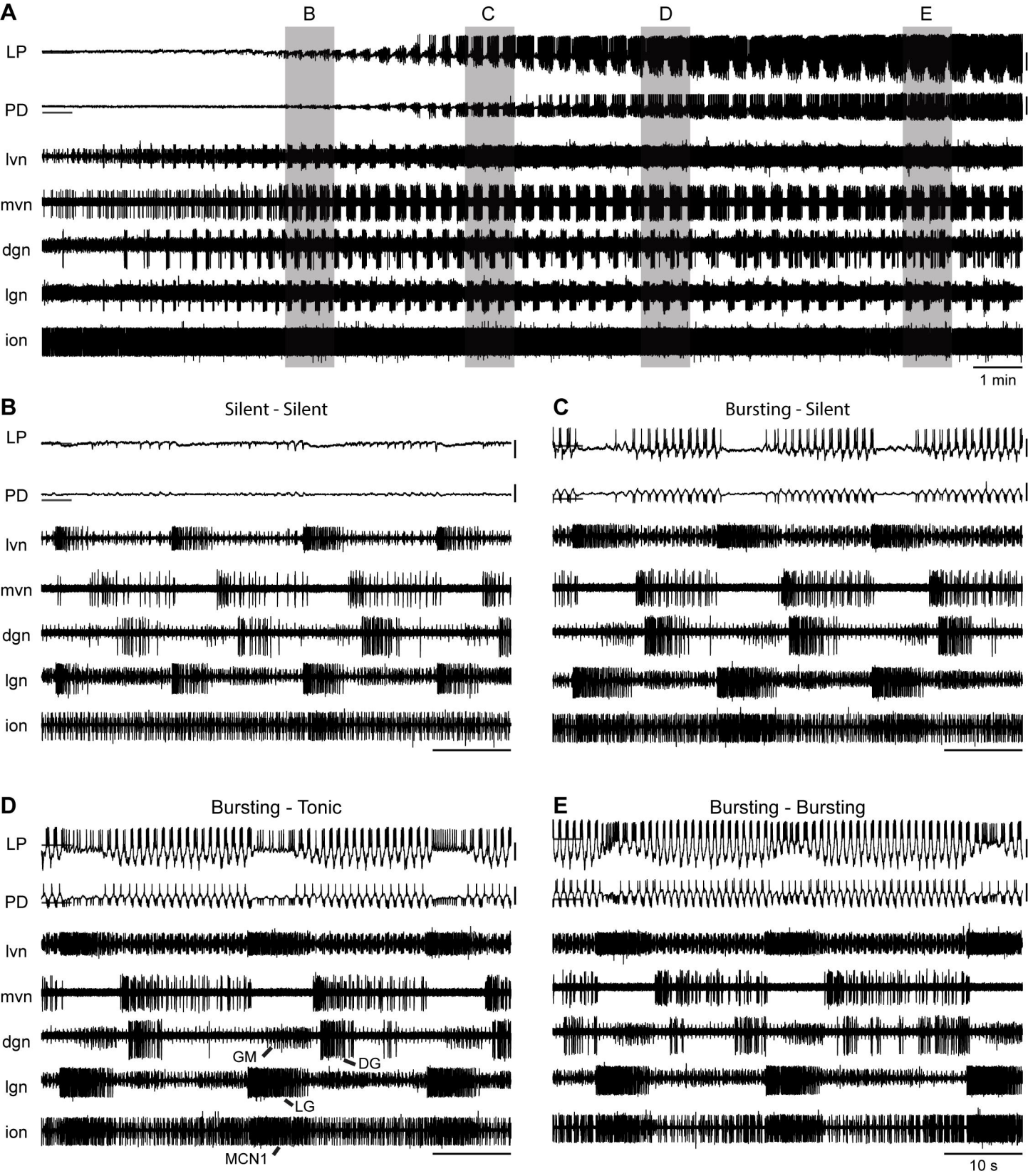
A
B
C
D
E
LP
PD
lvn
mvn
dgn
lgn
ion
1 min
B
Silent - Silent
C
Bursting - Silent
D
Bursting - Tonic
GM
DG
LG
MCN1
E
Bursting - Bursting
10 s

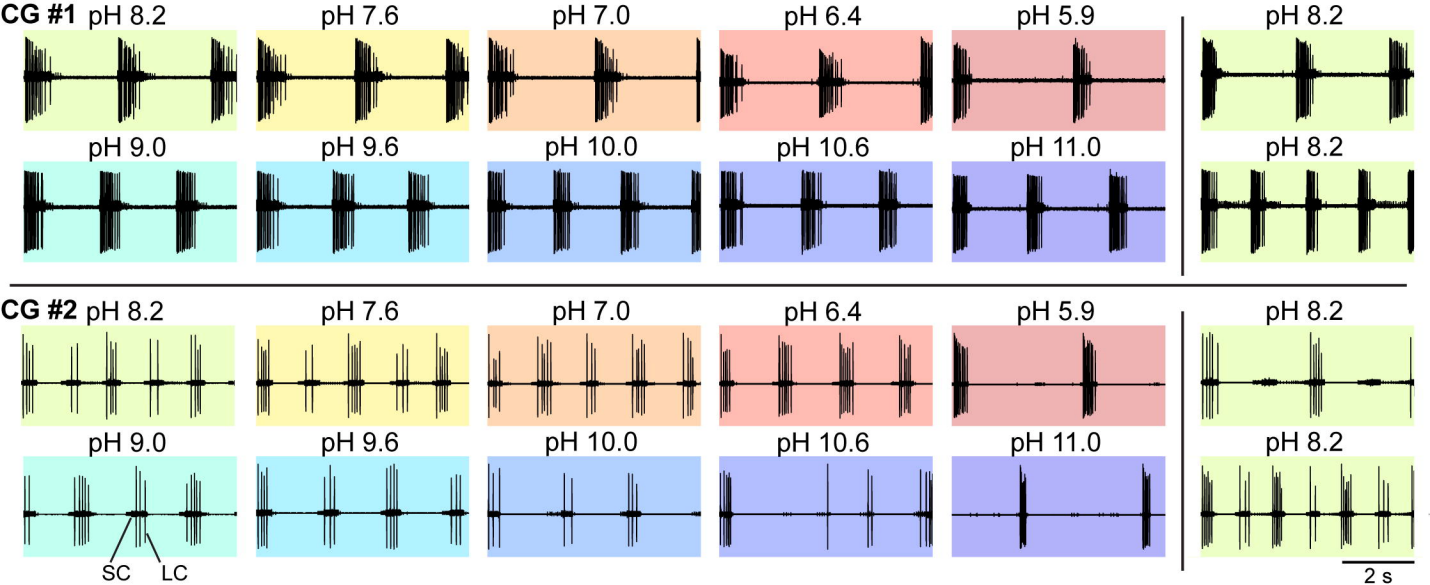
CG #1
pH 8.2
pH 7.6
pH 7.0
pH 6.4
pH 5.9
pH 8.2
pH 9.0
pH 9.6
pH 10.0
pH 10.6
pH 11.0
pH 8.2
CG #2
pH 8.2
pH 7.6
pH 7.0
pH 6.4
pH 5.9
pH 8.2
pH 9.0
pH 9.6
pH 10.0
pH 10.6
pH 11.0
pH 8.2
SC
LC
2 s

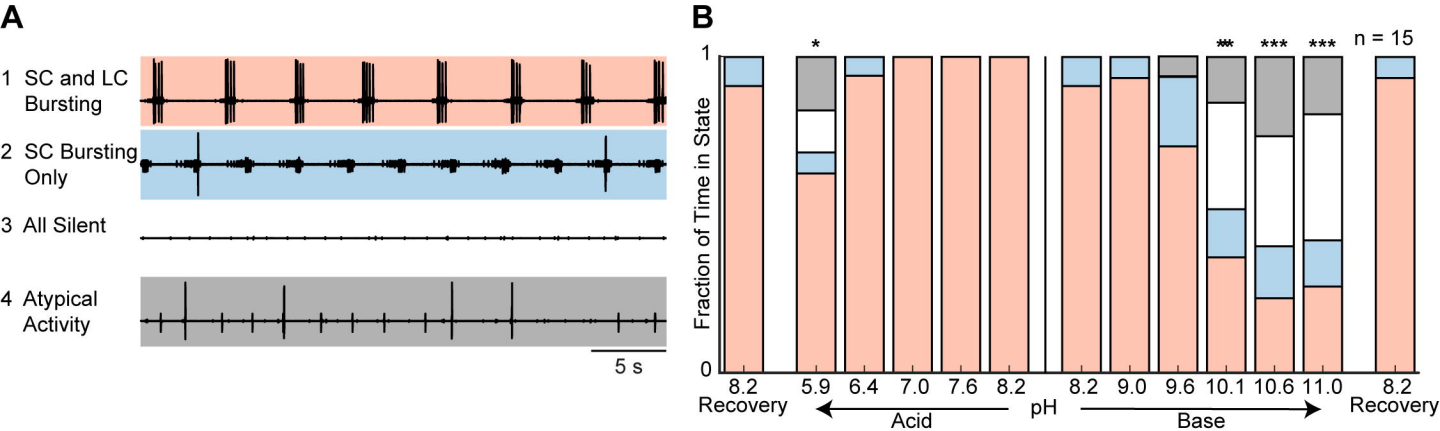
A
1 SC and LC Bursting
2 SC Bursting Only
3 All Silent
4 Atypical Activity
5 s
B
n = 15
Fraction of Time in State
1
0
*
***
***
***
8.2 Recovery
5.9
6.4
7.0
7.6
8.2
8.2
9.0
9.6
10.1
10.6
11.0
8.2 Recovery
Acid
pH
Base

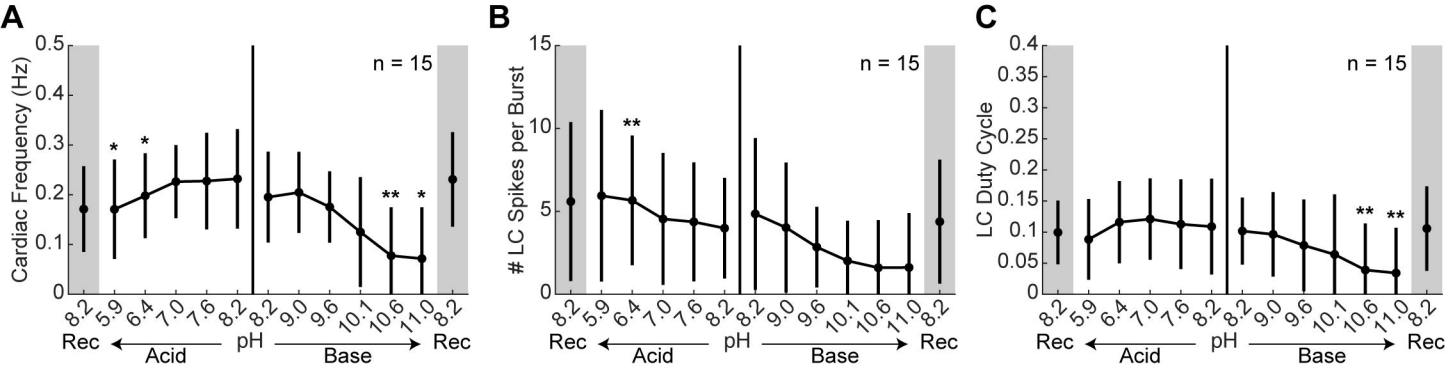
A
Cardiac Frequency (Hz)
n = 15
B
# LC Spikes per Burst
n = 15
C
LC Duty Cycle
n = 15
8.2
5.9
6.4
7.0
7.6
8.2
9.0
9.6
10.1
10.6
11.0
Rec
Acid
pH
Base
Rec

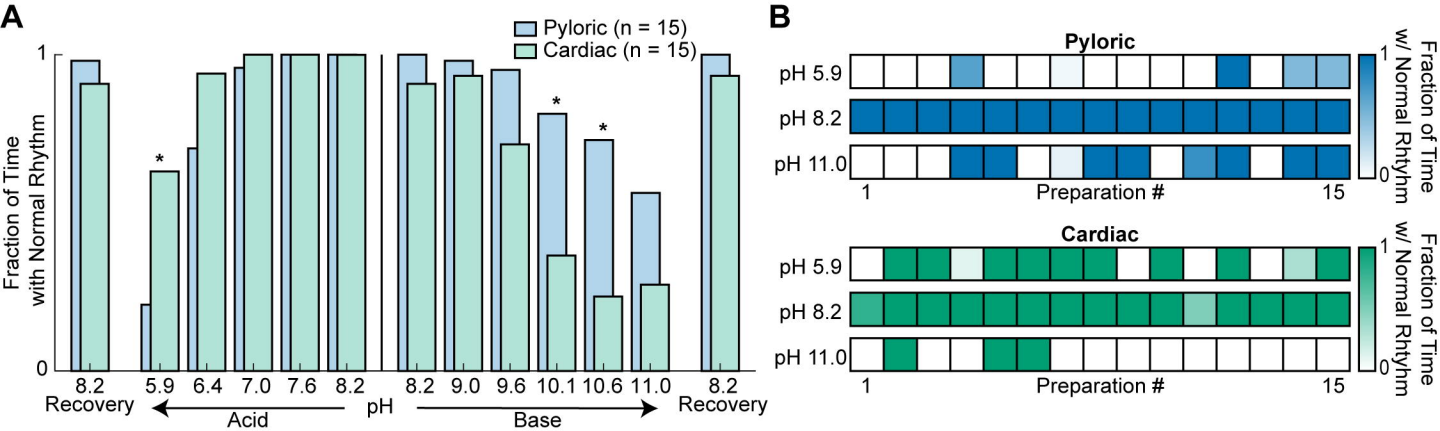
A
Pyloric (n = 15)
Cardiac (n = 15)
Fraction of Time with Normal Rhythm
1
0
*
*
*
8.2
Recovery
5.9
6.4
7.0
7.6
8.2
8.2
9.0
9.6
10.1
10.6
11.0
8.2
Recovery
Acid
pH
Base
B
Pyloric
pH 5.9
pH 8.2
pH 11.0
1
Preparation #
15
Fraction of Time w/ Normal Rhtyhm
1
0
Cardiac
pH 5.9
pH 8.2
pH 11.0
1
Preparation #
15
Fraction of Time w/ Normal Rhtyhm
1
0